

NUMERICAL INVESTIGATION OF NON-NEWTONIAN DRILLING FLUIDS DURING THE OCCURRENCE OF A GAS KICK IN A PETROLEUM RESERVOIR

F. F. Oliveira*, C. H. Sodr e and J. L. G. Marinho

Universidade Federal de Alagoas, Centro de Tecnologia,
Av. Lourival Melo Mota, Cidade Universit ria, Centro de Tecnologia,
CEP: 57000.000, Macei  - AL, Brasil.

Phone: + 55 21 82 32141260

*E-mail: ffreireoliveira@gmail.com

E-mail: chsodre@gmail.com; luis_gmarinho@yahoo.com.br

(Submitted: August 24, 2014 ; Revised: March 15, 2015 ; Accepted: May 6, 2015)

Abstract - In this work, a simplified kick simulator is developed using the ANSYS[®] CFX software in order to better understand the phenomena called kick. This simulator is based on the modeling of a petroleum well where a gas kick occurs. Dynamic behavior of some variables like pressure, viscosity, density and volume fraction of the fluid is analyzed in the final stretch of the modeled well. In the simulations nine different drilling fluids are used of two rheological categories, Ostwald de Waele, also known as Power-Law, and Bingham fluids, and the results are compared among them. In these comparisons what fluid allows faster or slower invasion of gas is analyzed, as well as how the gas spreads into the drilling fluid. The pressure behavior during the kick process is also compared. It is observed that, for both fluids, the pressure behavior is similar to a conventional leak in a pipe.

Keywords: Drilling; Kick; Well Control; CFX.

INTRODUCTION

The kick is a fluid flow from the petroleum reservoir into the well during the drilling process. It can happen if the differential pressure between the formation pressure and the fluid circulation (flow) pressure and the permeability of the rock are large enough. The main causes of kick are: mud weight less than formation pore pressure; lost circulation of drilling fluid; failure to keep the hole full with fluid while tripping; swabbing while tripping. (Grace, 2003; Avelar, 2008).

The main indications of a well kick are: sudden increase in drilling rate; increase in fluid volume at

the surface; pressure reduction due to the removal of the drilling column, this pressure reduction may generate negative pressure, allowing the formation fluid to flow into the well; gas, oil or water-cut mud; change in pump pressure. (Grace, 2003; Ajiienka and Owolabi, 1991).

Drilling Fluids

Drilling fluids are complex mixtures of solids, liquids, chemicals, and sometimes even gases. From the chemical point of view, they can assume aspects of suspension, colloidal dispersion or emulsion, depending on the physical state of the components

*To whom correspondence should be addressed

(Thomas, 2001). Also called mud, drilling fluids can often be defined as liquid compositions to help the process of drilling petroleum wells, and they depend on the particular requirements of each perforation (Barbosa, 2006).

Drilling fluids must be specified in order to ensure a fast and safe drilling process. According to Thomas (2001), the fluid should present some specific features, such as: it must be chemically stable; stabilize the walls of the well, mechanically and chemically; keep solids in suspension when at rest; accept any treatment, physical and chemical, and be pumpable; and finally, it should have cost compatible with the operation. Thomas (2001) also has written that the main functions of drilling fluids are to clean the bottom of the cuttings generated by the drill and transport them to the surface; generate hydrostatic pressure on the formations to prevent the influx of undesirable fluids (kick); stabilize the walls of the well, cool down and lubricate the drill string and drill bit.

Well Control

Kick can be controlled by circulating the invader fluid by employing a method of well control. The purpose of circulating an influx of gas is to bring the gas to the surface, allowing the gas to expand and preventing breakage of the well (Grace, 2003). Most methods of well control have as their basic principle to keep constant pressure into the bottomhole during kick removal. To prevent further inflows into the well, the bottomhole pressure should be kept equal to the formation pore pressure plus an added safety margin usually equivalent to the pressure drop in the annulus (Avelar, 2008).

According to the literature, the main methods of well control used today are: the Driller's Method, The Wait and Weight Method and Volumetric Methods.

The Driller's Method is simple and easily taught and understood by the drilling crew because it requires minimal calculation and consists of two steps of drilling fluid circulation.

The second method is more complex, requiring more precise calculations and only one circulation step (Grace, 2003; Avelar, 2008). The volumetric methods are applied when the circulation of the kick is not possible. These situations can occur when, e.g., the drill string is out of the well, the drill is a long distance from the bottom, drill jets are clogged or when there are mechanical problems with the circulation system. These methods are further divided into the Dynamic Volumetric Method and Static Volumetric Method (Avelar, 2008).

Non-Newtonian Fluids

Fluids can show large differences in behavior when under stress. Fluids that obey Newton's law, where the value of dynamic viscosity (μ) is constant are known as Newtonian fluids. If μ is a constant, shear stress is linearly dependent on the velocity gradient. The most common fluids are in this category (Sleigh and Noakes, 2009).

Fluids that do not obey Newton's law of viscosity are known as Non-Newtonian fluids. These are further divided into categories based on the relation between the shear stress and the rate of shear strain of the fluid. Figure 1 shows these categories.

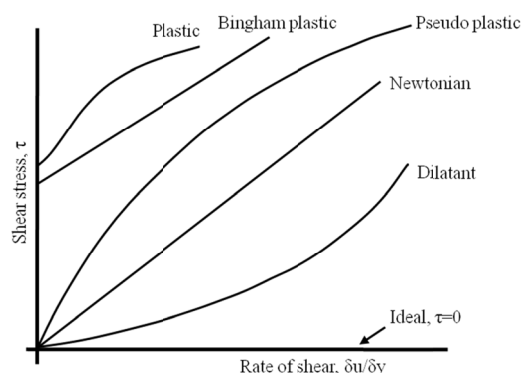


Figure 1: Shear stress vs. Rate of shear strain. Source: Sleigh and Noakes (2009).

Fluids with Rheological behavior of Bingham or Ostwald de Waele compose the majority of drilling fluids used in drilling oil wells, since they have important rheological characteristics for gravels removal.

The Bingham model, or ideal plastic, requires theoretically that a minimum shear stress, τ_L , be applied to produce some shear deformation. This minimum shear stress is called the yield stress and, when the fluid is subjected to a shear stress less than τ_L , theoretically it behaves as a solid. The mathematical expression that defines the Bingham fluid is given by Equation (1) (Machado, 2002),

$$\begin{aligned} \tau &= \mu_p \gamma + \tau_L & \text{for } \tau > \tau_L \\ \gamma &= 0 & \text{for } \tau \leq \tau_L \end{aligned} \quad (1)$$

where μ_p , γ and τ_L , represent plastic viscosity, rate of shear and yield stress, respectively.

The apparent viscosity is given by Equation (2):

$$\mu_a = \mu_p + \frac{\tau_L}{\gamma} \quad (2)$$

The Ostwald de Waele model, also known as the Power-Law model, shows the relation of shear stress, τ defined as:

$$\tau = K(\dot{\gamma})^n \quad (3)$$

where K and n are the rheological parameters, known as *consistency index* and *behavior index*, respectively (Machado, 2002).

The Power-Law fluids are divided into two categories according to their index behavior value. For n values smaller than one and greater than zero, these fluids are called *pseudoplastics*. If n is greater than 1 they are called *dilatants*. When the value of n is unity, the fluid behaves like a Newtonian fluid. The behavior of Power-Law fluids can also be analyzed by the apparent viscosity variation with shear rate. The apparent viscosity of the fluid can be determined through Equation (4) (Machado, 2002).

$$\mu_a = K(\dot{\gamma})^{n-1} \quad (4)$$

Objective and State of the Art

This paper aims to understand what happens in the bottomhole of petroleum wells during the drilling process, offering a tool that can be used to predict the behavior of some important variables like pressure and amount of formation fluid that can invade the pit.

The literature is very poor in articles dealing with this topic, mainly due to the lack of information that can be used to validate the results and the complexity and specificity of oil well drilling procedures that are performed mostly by large companies that do not make public their working methods. Thus, research devoted to this topic is welcome.

METHODOLOGY

Physical Problem Description (Case Studied)

The case study was to analyze the kick during drilling of an oil well. A kick simulator was developed. Figure 2 shows the sketch of an oil well being drilled. For the simulation of the kick, the gas inlet is located at the end of the stretch without casing of an oil well (drilled in reservoir rock). The fluid (black arrows in the detail of Figure 2) along with the gas (green arrows, in the detail of Figure 2) flows in the annular region in an upward two-phase flow. The

study was performed by analyzing transient two-phase flow profiles.

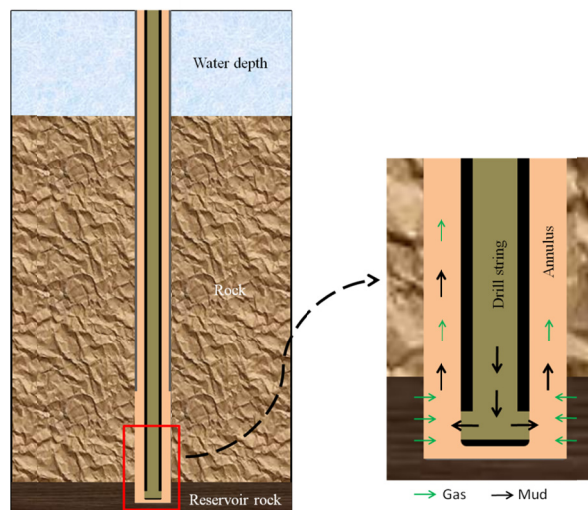


Figure 2: Representation of the well and detail of the final stretch.

Description of Geometry of the Studied Domain

After making the above considerations, the geometry shown in Figure 3 was The well studied is located in the middle of the reservoir, it was assumed that the gas is equally distributed at the entrance. Considering the symmetry of the well, only a slice of the tube was taken to perform the simulation. What happens in this slice approximately represents the whole region. This was required in order to simplify the domain to be studied and especially to reduce the computational effort. A section of 45 degrees of the tube was modeled and, assuming symmetry, the result obtained in this region can be extrapolated to the entire area. The section is shown in Figure 3 A and B.

It is also known that an oil well, especially in the pre-Salt region, frequently reaches depths exceeding five thousand meters in the final phase of drilling. A modeling spanning that length would be impractical due to the computational effort required. Tests were performed in order to define the length that would stretch the length of the desired pipe. After some tests, it was concluded that a tube about 20 meters long would be suitable to represent what would happen in the pit at the time of the studied phenomenon designed using the ANSYS® ICEM 13.0 CFD software. The dimensions of the geometry are given in Table 1 and Figure 3 C. The mesh used was a structured model with 237 476 predominantly hexahedral elements.

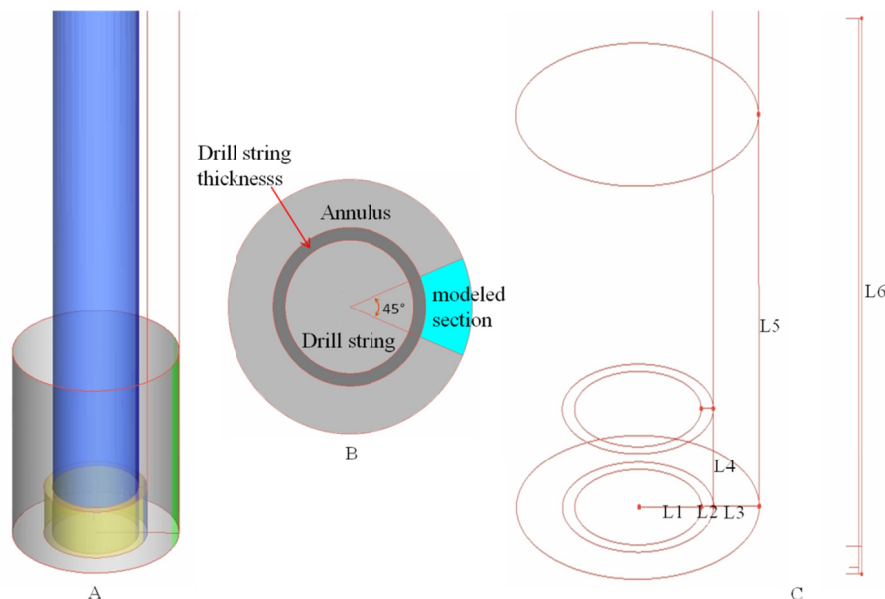


Figure 3: Dimensions of the geometry used in the model: (A) Three-dimensional representation; (B) Detail of the modeled section; (C) Size.

Table 1: Features of the developed geometry.

Dimension	Value (in)	Value (cm)	Description
$L1 = d_i / 2$	2.1	5.334	Inner radius of drill string
$L2$	0.4	1.016	Drill string thickness
$L3$	1.5	3.81	Annular length
$L4$	2.5	6.35	Drilling fluid inlet height
$L5 = H_{res}$	10	25.4	Gas inlet height

Source: AVELAR (2008); Author

Drilling Fluids and Natural Gas Used

The behavior of nine drilling fluids was analyzed during the kick process, all non-Newtonian fluids, five being Power-Law fluids (all pseudoplastic) and four Bingham fluids. The parameters of each fluid are shown in Table 2.

Table 2: Rheological properties of drilling fluids.

Parameters	Power-Law		Bingham	
	K (Pa.s ⁿ)	n	τ_L (Pa)	μ_p (Pa.s)
Fluid 1	2.4	0.376	5.966	0.012
Fluid 2	0.855	0.549	3.527	0.019
Fluid 3	0.42	0.634	2.612	0.017
Fluid 4	1.154	0.543	3.561	0.029
Fluid 5	2.096	0.468		

Source: WALDMANN (2012)

The natural gas found during drilling may show values above 90% methane in its composition (Lee *et al.*, 1966). Thus, in this study, in order to simplify the modeling it was considered that the composition

of natural gas consists mostly of methane. The main properties of this gas are shown in Table 3.

Table 3: Methane gas properties.

Properties	Value
Molar mass	0.016 kg/mol
Density	223.7 kg/m ³
Dynamic viscosity	2.8242×10^{-5} Pa.s
Reference temperature	365 K
Reference pressure	4.9977×10^7 Pa

Source: PEACE (2013); LEE *et al.* (1966)

Mathematical Model

The mathematical model used in this work was the Finite Volume Model (FVM), which is already embedded in the software used. FVM is a method for representing and evaluating partial differential equations in the form of algebraic equations. Values are calculated at discrete places on a meshed geometry as fluxes at the surfaces of each finite volume, that is, the small volume surrounding each node point on a mesh. The timestep was 0.1 s with up to ten iterations per timestep and the k- ϵ turbulence model was utilized in the simulations.

Modeling Considerations

The following considerations were made, with regard to the properties of the fluids involved:

- All drilling fluids are considered incompressible;

- The variation of the gas compressibility was considered to be very small, and therefore neglected;
- The temperature variation in the evaluated stretch was neglected;
- The physicochemical properties of drilling fluids and gas remained constant in the analyzed section;
- The drilling fluid and gas inlet pumping speeds were considered constant in the analyzed time interval.

Initial Conditions

The initial condition of the well represents a normal drilling situation, with known constant flow rate of circulating drilling fluid and without the presence of gas within the well. In this case, the drilling velocity v_{le} at the entrance of the well is calculated by Equation (5),

$$v_{le} = \frac{\dot{Q}_l}{\pi d_i^2 / 4} \quad (5)$$

where \dot{Q} is the volumetric flowrate of drilling fluid injected into the well, and d_i is the diameter of the drill string.

The pressure ($p_{formation}$) at the point where the entrance of drilling fluid occurs is given by Equation (6).

$$p_{formation} = SIDPP + \rho_l g D_p \quad (6)$$

where $SIDPP$ is the shut-in drill pipe pressure; ρ_l is the density of the drilling fluid; g is the acceleration of gravity, and D_p is the depth of the well at that point.

After a determined period of time, a formation with pressure above the one exerted by the drilling fluid is reached, the gas from this formation begins to enter the well. The pressure of this porous formation was estimated to be 10% greater than that exerted by the drilling fluid at the same point, which was also calculated by Equation (6).

During the entry of gas into the well, the fluid pumping conditions remain unchanged and the velocity of the liquid at the entrance of the well can be calculated by Equation (5). In this step, the input flow of gas is determined by the equation of permanent radial flow in porous medium for compressible fluids, shown in Equation (7) (Rosa *et al.*, 2006).

$$\dot{Q}_g = \frac{2\pi K_{res} H_{res} (p_{formation} - p_{bottom})}{\mu_g \ln\left(\frac{d_{res}}{d_e}\right)} \quad (7)$$

The entrance velocity of the gas into the well is calculated by Equation (8).

$$v_{ge} = \frac{2\pi K_{res} H_{res} (p_{formation} - p_{bottom})}{\mu_g \ln\left(\frac{d_{res}}{d_e}\right)} \frac{1}{\pi d_e H_{res}} \quad (8)$$

where K_{res} and H_{res} are the permeability and reservoir height, respectively, $(p_{formation} - p_{bottom})$ is the differential pressure in the bottomhole; μ_g is the gas viscosity; d_{res} and d_e are the diameters of the reservoir and the well, respectively; $\pi d_e H_{res}$ is the surface area of the gas entrance. The gas density is calculated using Equation (9).

$$\rho_g = \frac{(p_{bottom} + p_{atm})M}{Z'RT} \quad (9)$$

where p_{bottom} and p_{atm} are the pressures in the bottomhole and the atmospheric pressure, respectively, M is the molecular mass of the gas, Z' is the compressibility factor, R is the universal gas constant, T is the temperature in the bottomhole.

The gas viscosity (μ_g) given in micropoise was calculated by Equation (10), which was developed by Lee *et al.* (1966).

$$\mu_g = K' \exp\left[X' \rho_g^{Y'}\right] \quad (10)$$

where

$$K' = \frac{(7.77 + 0.063M)T^{1.5}}{122.4 + 12.9M + T} \quad (11)$$

$$X' = 2.57 + \frac{1914.5}{T} + 0.0095M \quad (12)$$

$$Y' = 1.11 - 0.04X' \quad (13)$$

where ρ_g is the gas density, g/cm^3 ; T is the local temperature given in °R and M is the molecular weight of the gas, in g/mol. Other parameters and

initial conditions used in the simulations are summarized in Table 4.

Table 4: Parameters used in simulations.

Parameter	Value (SI Units)
Total depth of the well	3 600 m
Thickness of the water depth	1 000 m
Height of the well	20.32 m
Well diameter	0.2032 m
Outside diameter of the drill string	0.1219 m
Thickness of the drill string	0.01016 m
SIDPP	3.1026×10^6 Pa
Density of the drilling fluid	1 199 kg/m ³
Surface temperature	300 K
Pressure on the surface	101 325 Pa
Geothermal gradient	0.025 K/m
Reservoir permeability	9.8692×10^{-13} m ²
Reservoir height	0.254 m
Reservoir diameter	1 000 m
Acceleration of gravity	9.8066 m/s ²
Pressure in the bottomhole	4.9977×10^7 Pa
Temperature in the bottomhole	365 K
Speed of drilling fluid in the inlet	3.9831 m/s
Speed of the gas at the inlet	0.1838 m/s

Source: AVELAR (2008); PERRY (1999), REID *et al.* (1986)

Data Acquisition

Several simulations were performed and the results were analyzed at four points. The locations of these points are presented in Table 5 and Figure 4.

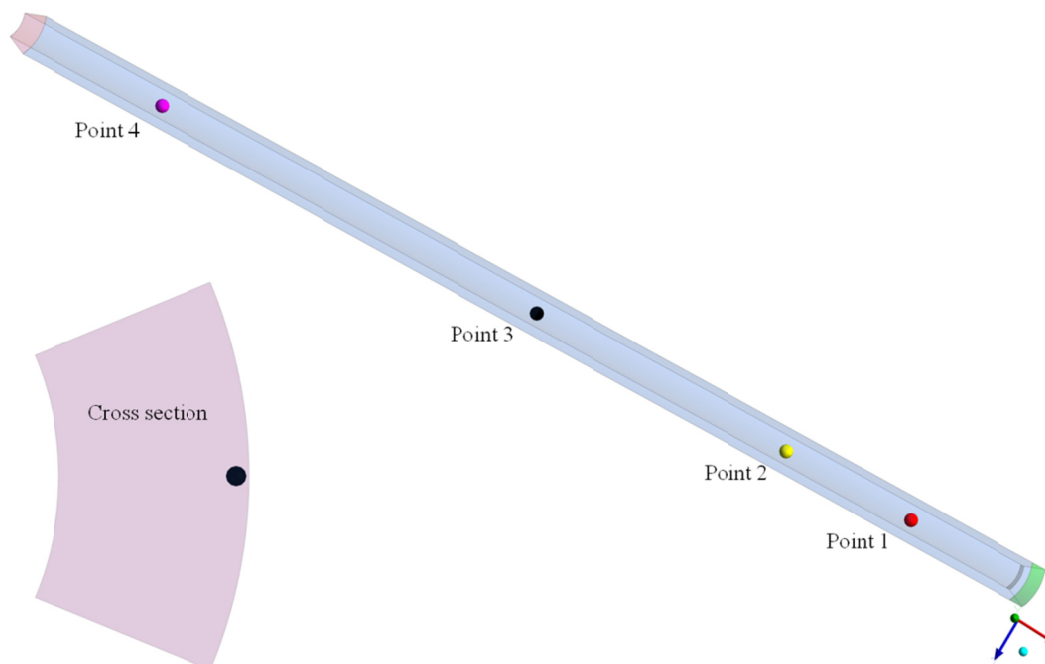


Figure 4: Location of data acquisition points.

Table 5: Points for data acquisition.

Point/coordinates	X (cm)	Y (cm)	Z (cm)
Point 1	9.906	254	0
Point 2	9.906	508	0
Point 3	9.906	1 016	0
Point 4	9.906	1 778	0

RESULTS AND DISCUSSION

Influence of Viscosity in Power-Law Fluids

Five Power-Law fluids were analyzed, all of the pseudoplastic type with different indices of consistency and behavior. The characteristics of each fluid are presented in Table 2. To compare the behavior of each fluid, five simulations were performed; only the drilling fluid was replaced, keeping all other settings unchanged.

Figures 5 and 6 show the comparison of the volume fraction of the drilling fluid as a function of the time at the points 2 and 4, respectively. Analyzing the graph in Figure 5, it can be seen, at the beginning of the simulation, that the third fluid allowed invasion of gas faster than the other fluids, causing a decrease in the concentration of the drilling fluid more quickly at the observed point. This could be explained because this fluid has the lowest viscosity in comparison to the others.

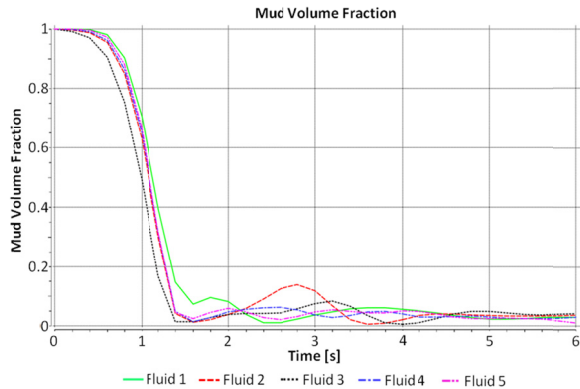


Figure 5: Volumetric fraction of drilling fluids (Power-Law) at the point 2.

Figure 6 shows the volumetric fraction of drilling fluids at the point 4. At this point, the differences in gas invasion in the drilling fluids are very little, suggesting that the invading gas reaches this point almost at the same time for all fluids analyzed.

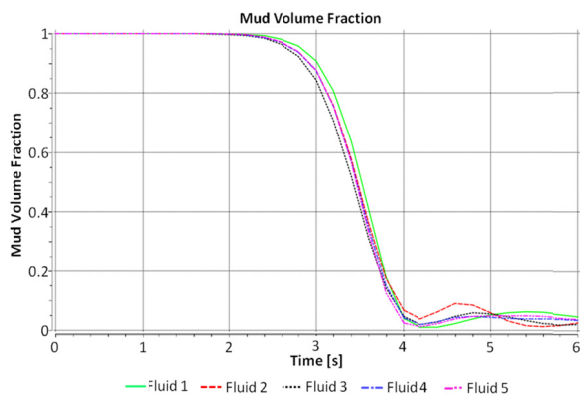


Figure 6: Volume fraction of drilling fluids (Power-Law) at the point 4.

Influence of Plastic Viscosity in Bingham Fluids

The characteristics of each Bingham fluid analyzed are shown in Table 2. Four Bingham fluids with different plastic viscosities and flow limits were analyzed. To compare the behavior of each fluid, four simulations were performed and only the drilling fluid was replaced, keeping all other settings unchanged. The $k-\epsilon$ turbulence model was also used for these simulations.

Figures 7 and 8 show the fluid density behavior at points 3 and 4, respectively, for Bingham fluids. Figure 7 shows the density profiles at point 3. The decrease of density for Bingham fluid #4 occurs at a later time than for the other fluids. This result shows that, for fluid with higher plastic viscosity, the gas progress is slow.

Figure 8 shows the density profiles at the point 4. The same pattern of density drop with time was kept with a slight decrease in time for the Bingham fluid #4.

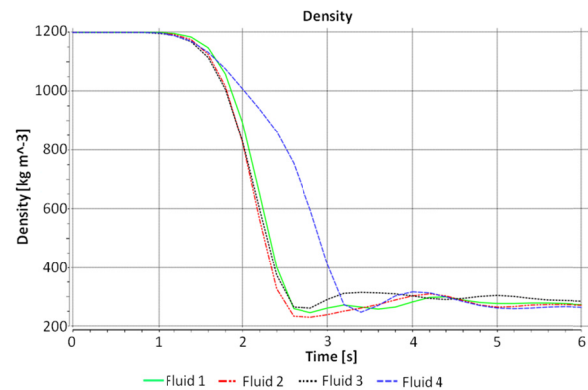


Figure 7: Density of drilling fluids (Bingham) at the point 3.

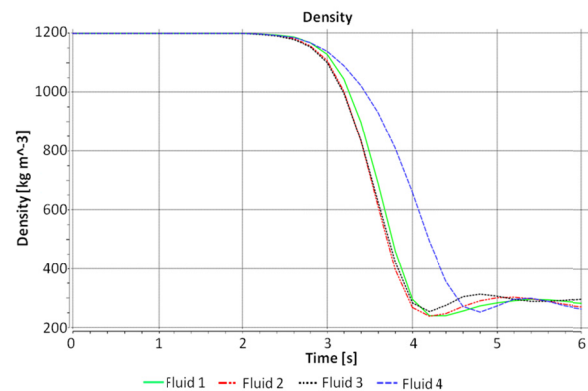


Figure 8: Density of drilling fluids (Bingham) at the point 4.

Influence of Fluid Type: Power-Law vs. Bingham

Two types of non-Newtonian fluids with different rheological behavior were used: the ideal plastic or Bingham fluid and Ostwald de Waele fluid. To compare the behavior of these, two simulations were performed using the Bingham fluid #1 and Power-Law fluid #1; all properties of these fluids are described in Table 2. The graph in Figure 9 shows the variation of the volumetric fraction of methane invading the drilling fluid for both Bingham and Power-Law fluids at the point 1. It can be noted that the fluids behave identically in the first moments until they reach the maximum concentration of methane. From that point both graphs begin to show mismatch.

The graph in Figure 10 shows the variation of the volumetric fraction of methane invading drilling at the point 4. At this point, the concentration of me-

thane in the simulation with a Bingham fluid can reach the maximum value at slightly earlier time than that observed with the Power-Law fluid.

Considering the cases studied here, the result shows that the gas propagates more quickly when the drilling fluid has ideal plastic rheological behavior (Bingham fluid).

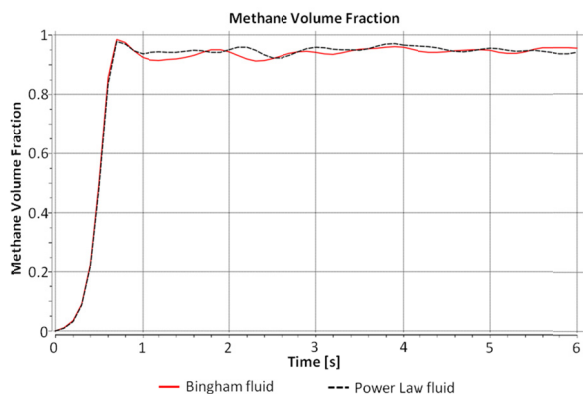


Figure 9: Methane volume fraction at the point 1.

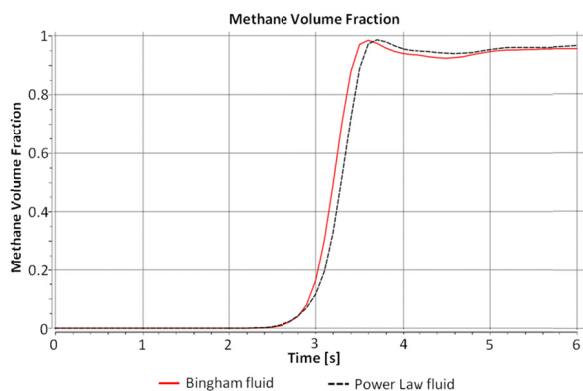


Figure 10: Methane volume fraction at the point 4.

Figure 11 shows the pressure variation at the point 3. When the gas invades the well, the pressure drops abruptly, causing a kind of instant vacuum and reaching its lowest value.

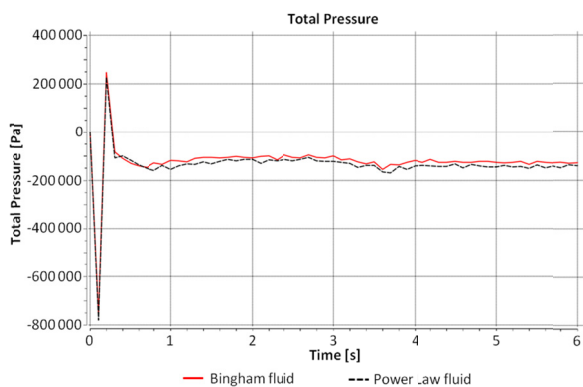


Figure 11: Pressure variation at the point 3.

Then it goes back up to a level close to the initial reference pressure and further back to an intermediate level which tends to stabilize over time.

The pressure behavior shown in Figure 11 is similar to the one observed in the profile of a conventional leak in a pipe. It is also noted that the pressure drop is almost equal for both fluids.

CONCLUSION

Well drilling in areas with high pressures and temperatures are becoming more common, although it requires high technology. One of the most important points in the drilling process is controlling the pressure within the well. If this control fails, the formation fluids can invade the well, causing the kick.

In this work, a simplified kick simulator was developed to aid the analysis, through graphics, of the dynamic behavior of some variables, such as volume fractions of both drilling fluid and gas, density of the gas-liquid mixture in the well and pressure.

During the analysis with Power-Law fluids, it was observed that fluid #3, being less viscous, initially allowed faster gas invasion, causing a decrease in the concentration of the drilling fluid more quickly at the observed point. For the analyses with Bingham fluids, it was noted that the fluid #4, with higher plastic viscosity, allowed slower advance of the invading gas.

Considering the cases analyzed here, the comparison between the Power-Law fluid and Bingham fluid showed that the gas spreads quickly when the drilling fluid has ideal plastic rheological behavior, i.e., is a Bingham fluid.

For the pressure variable, it was observed that, when gas invades the well, the pressure drops sharply and reaches its lowest value; then it goes back up to a level close to the initial pressure and back to an intermediate level, which tends to stabilize over time. This behavior is similar to a conventional leak in a pipe. It was further observed that the pressure drop was almost the same when the two kinds of fluids were compared.

As has been said, there is a lack of information about this topic in the literature that can be used to compare the results obtained here. It is expected that, in the future, there will be more papers related to the subject and such comparisons can be made, thus contributing positively to the decisions of the engineer responsible for the drilling. It would also contribute to an improvement in training and staff development, as well as a better understanding and interpretation of the phenomena occurring in the field.

NOMENCLATURE

d_e	Well outer diameter (m)
d_i	Inner diameter of drill string (m)
D_p	depth of the well (m)
d_{res}	Reservoir diameter (m)
g	acceleration of gravity ($m.s^{-2}$)
H_{res}	Reservoir height (m)
K	consistency index ($kg.m^{-1}s^{-2}s^n$)
K'	LEE equation parameter ---
K_{res}	Reservoir permeability (m^2)
M	Molecular mass of the gas ---
n	behavior index ---
p_{atm}	Atmospheric pressure (Pa)
$p_{formation}$	Formation pressure (Pa)
P_{bottom}	Bottomhole pressure (Pa)
\dot{Q}_g	Flow of gas ($m^3.s^{-1}$)
\dot{Q}_l	Flow of drilling fluid ($m^3.s^{-1}$)
R	Universal gas constant ($m^2.s^{-2}.T^{-1}$)
$SIDPP$	shut-in drill pipe pressure (Pa)
T	Bottomhole temperature (K)
v_{ge}	Velocity of the gas in the entrance ($m.s^{-1}$)
v_{le}	Velocity of the drilling fluid in the entrance ($m.s^{-1}$)
X	Cartesian coordinate (m)
X'	LEE equation parameter ---
Y	Cartesian coordinate (m)
Y'	LEE equation parameter ---
Z	Cartesian coordinate (m)
Z'	Compressibility factor ---

Greek Letters

γ	Shear stress rate (s^{-1})
μ_a	Apparent viscosity (Pa.s)
μ_g	Gas viscosity (Pa.s)
μ_p	Plastic viscosity (Pa.s)
ρ_g	Gas density ($kg.m^{-3}$)
ρ_l	density of the drilling fluid ($kg.m^{-3}$)
τ	Shear stress (Pa)
τ_L	Yield stress (Pa)

REFERENCES

Ajienka, J. A. and Owolabi, O. O., Application of mass balance of kick fluid in well control. Journal

- of Petroleum Science and Engineering, 6(2), 161-174 (1991).
- Avelar, C. S., Well Control Modeling: A Finite Difference Approach. Master Thesis, State University of Campinas, Campinas, Brasil (2008).
- Barbosa, M. I. R., Bentonites Treated with Polymeric Additives for Application in Drilling Fluids. Master Thesis Federal University of Campina Grande, Campina Grande, Brasil (2006).
- Grace, R. D., Blowout and Well Control Handbook. With contributions by Cudd, B. *et al.* Elsevier Science, USA (2003).
- Lee, A. L., Gonzalez, M. H. and Eakin, B. E., The viscosity of natural gases. Journal of Petroleum Technology, 18(8), 997-1000 (1966).
- Machado, J. C. V., Reologia e escoamento de fluidos: Ênfase na indústria do petróleo. Interciência, Rio de Janeiro (2002). (In Portuguese).
- Peace Software, Some scientific and engineering data online. 2013. Available in: <http://www.peacesoftware.de/einigewerte/einigewerte_e.html> (Accessed: October 10, 2013).
- Perry, R. H., Perry's Chemical Engineers' Handbook. 7th Ed. McGraw-Hill, USA (1999).
- Reid, R. C., Prausnitz, J. M. and Poling, B. E., The Properties of Gases and Liquids. 4th Ed. Singapore, Mc-Graw-Hill (1986).
- Rosa, A. J., Carvalho, R. S. and Xavier, J. A. D., Engenharia de Reservatórios de Petróleo. Interciência, Rio de Janeiro (2006). (In Portuguese).
- Sleigh, A. and Noakes C., An introduction to fluid mechanic: Fluid mechanics and fluid properties. School of Civil Engineering, University of Leeds, (2009). Available in: <http://www.efm.leeds.ac.uk/CIVE/CIVE1400/Section1/Fluid_mechanics.htm> (Accessed: January 2, 2014).
- Thomas, J. E., Fundamentos de Engenharia de Petróleo. Interciência, Rio de Janeiro (2001). (In Portuguese).
- Waldmann, A. T. A., Martins, A. L., Souza, E. A., Loureiro, S. A., Andrade, A. R., Scheid, C. M., Calçada, L. A., Moreno, R. Z. and Dannenhauer, C. E., R&D Efforts to Control, Monitor and Identify Drilling Fluid Invasion Into Reservoir Rocks. In: 1st International Conference on Upstream Engineering and Flow Assurance, a Part of the 2012, AIChE Spring Meeting, Texas (2012).